THE COMPARISON OF HYDROGEN DIFFUSION CHARACTERISTICS IN DIFFERENT KINDS OF TRIP STEELS

KULOVÁ Taťána[1], SOJKA Jaroslav[1], VÁŇOVÁ Petra[1], SOZAŃSKA Maria[2]

[1]VSB - Technical University of Ostrava, Faculty of Metallurgy and Materials Engineering, Ostrava, Czech Republic, EU, tatiana.kulova@vsb.cz
[2]Silesian University of Technology, Katowice, Poland, EU

Abstract

The presented paper is devoted to the comparison of hydrogen diffusion characteristics in three different kinds of TRIP steels (with higher phosphorus content, higher aluminum content and higher silicon content). The steels were tested in as-received state after standard heat treatment including two step annealing - an intercritical annealing and an annealing in the range of bainitic transformation and in states after 5 % and 10 % tensile deformation. Steel microstructures were analyzed by light microscopy, scanning electron microscopy and X - ray diffraction. Hydrogen diffusion characteristics were electrochemically measured by Devanathan-Stachurski method with a double cell separated by steel in the form of a thin membrane. Exit sides of the steel membrane were palladium coated to prevent from hydrogen atom recombination during permeation experiments. Hydrogen diffusion coefficients were calculated using the „time lag“ method. The lowest values of hydrogen diffusion coefficients were recorded in the TRIP steel with higher aluminum content, while the highest values were observed in the TRIP with higher phosphorus content. Phosphorus probably enhances hydrogen diffusion in steel. Very high sub-surface hydrogen concentrations were observed also in the TRIP steel with higher phosphorus content.

Keywords: TRIP steel, hydrogen diffusion characteristics, electrochemical permeation method

1. INTRODUCTION

The need to reduce the mass of automobile “body in white” components whilst meeting strict safety standards has spurred increased interest in advanced high strength steel (AHSS) grades. TRIP steels (Transformation Induced Plasticity) are one of AHSS with a microstructure of ferritic matrix together with grains of carbide-free bainite, and retained austenite [1]. The latter transforms fully or partially under mechanical load to martensite (TRIP effect) and contributes to improved strain hardening and postponed necking. The combination of strength and ductility allow TRIP steels to absorb large amounts of energy before rupture occurs [2]. The properties of TRIP steels depend on an optimal chemical composition, and it is essential to include elements that inhibit cementite and/or carbide precipitation to ensure a sufficient quantity of retained austenite (RA) remains in the steel microstructure at ambient temperature. TRIP steels were initially based on the C-Mn-Si chemical composition. The main contribution of silicon is that it significantly increases carbon activity, especially in ferrite, reduces carbon solubility in ferrite and thus provides an efficient enrichment austenite in carbon during heat treatments. Another benefit of silicon is the ability to suppress the formation of cementite especially in the area of bainitic transformation. Due to the fact that silicon may cause serious difficulties during hot-dip galvanizing, this element is often partially or totally replaced by aluminum. Another benefit from the presence of aluminum is that Al accelerates the bainite formation, which is very important in the continuous industrial production. Aluminum, on the other hand, increases martensite start (M_s) temperature and destabilizes retained austenite in this way [3]. Variants of TRIP steels have also been developed with high phosphorus content, again to improve conditions of hot-dip galvanizing and to facilitate retained austenite stabilization. Appropriate amount of the retained austenite in the TRIP steels (10 - 15 %) is however essential for the achievement of optimal mechanical properties [4], [5]. One of the basic technological demands of TRIP steels is easy hot-dip galvanizing to ensure they have corrosion resistance [6]. A pre-treatment process, e.g.,

acid pickling in different acids (preferentially in HCl), precedes hot-dip galvanizing. This operation represents a risk from hydrogen embrittlement, as hydrogen can enter the steel during the acid pickling process. In general, a high resistance of TRIP steels to hydrogen embrittlement is assumed because of the higher retained austenite content. The retained austenite in steels is favorable, in that it can form traps that can strongly bind hydrogen [7].

In this work the hydrogen diffusion characteristics of three variants of TRIP steel were compared. The hydrogen diffusion characteristics were measured by the electrochemical permeation method of hydrogen. The steels were studied in three different states: in the as-received state (after both hot and cold rolling and a subsequent heat treatment) and furthermore after 5 % and 10 % tensile deformation to change both mechanical properties and microstructure of the steel.

2. MATERIALS AND EXPERIMENTAL TECHNIQUES

Three different TRIP 800 steels with guaranteed minimum yield strength of 420 MPa and minimum tensile strength of 800 MPa were used in our experimental study. The first alloy (designated as Sample A hereafter) was a sheet of C-Mn-Si TRIP steel with a thickness of 1.5 mm produced under laboratory conditions using the laboratory rolling mill at the Faculty of Metallurgy and Materials Engineering (FMME) VSB (Technical University of Ostrava) in the Czech Republic (FMME VSB - TUO). The second alloy (designated as Sample B hereafter) was a sheet of C-Si-Mn-Al TRIP steel with the same thickness as Sample A. Sample B was also prepared in the laboratory at FMME VSB - TUO. The third alloy (designated as Sample C hereafter) was a sheet of C-Si-Mn-P TRIP steel with the same thickness as Sample A and Sample B and Sample C was also prepared in the same laboratory. The chemical composition of the three variants TRIP steel is given in **Table 1**.

Table 1 Chemical composition of the studied TRIP steels (wt. %)

Sample	C	Mn	Si	P	S	Cr	Mo	Cu	Al
A	0.20	1.48	1.48	0.014	0.004	0.17	0.01	0.06	0.06
B	0.21	1.57	1.05	0.013	0.005	0.16	0.01	0.07	0.54
C	0.20	1.50	1.50	0.050	0.005	0.16	0.01	0.06	0.006

Generally, the heat treatment of the TRIP steels consists of the five stages shown in **Figure 1**: rapid heating, self intercritical annealing, rapid cooling, isothermal endurance at the temperature of the bainitic transformation, and the last stage is cooling to room temperature. Details concerning steel manufacturing and its heat treatment can be found in [8].

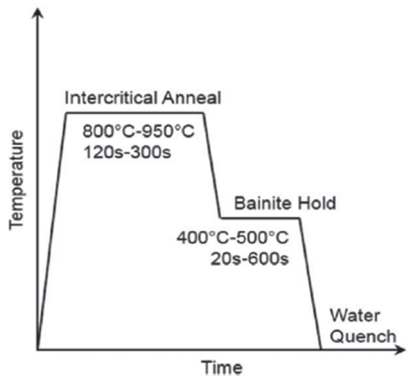

Figure 1 General scheme of heat tretment for TRIP steels

Mechanical properties and content of retained austenite of the studied TRIP steels are given in **Table 2** in as-received state.

Table 2 Mechanical properties of the studied TRIP steels in as-received state

Sample	Yield strength (MPa)	Tensile strength (MPa)	Elongation at fracture (%)	Retained austenite content (%)
A	440	890	29.5	11.0 ± 2.0
B	425	880	29.5	13.0 ± 2.0
C	401	925	27.2	14.9 ± 2.0

Steel structures were observed using light microscopy (LM) and scanning electron microscopy (SEM) [8]. Retained austenite (RA) content was determined by means of X-ray analysis using Co K_α source (λ = 0.17902 nm). From the point of view of LM and SEM the steel microstructure consisted of ferrite and bainite only. In some micrographs, presence of martensite was also revealed using SEM. Examples of the microstructure of the studied TRIP steel are shown in **Figure 2a, b, c, d** for the as-received state and for the state after 10 % tensile deformation.

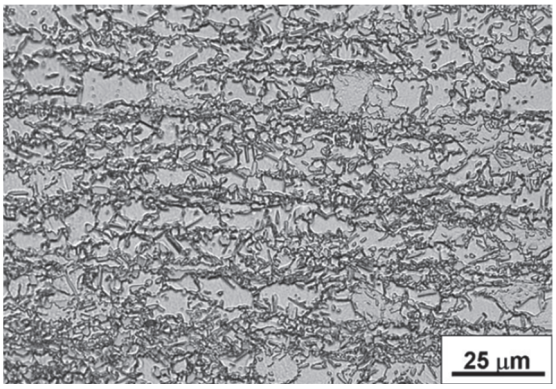

a) Microstructure of TRIP steel Sample A in as-received state (LM with Nital etch)

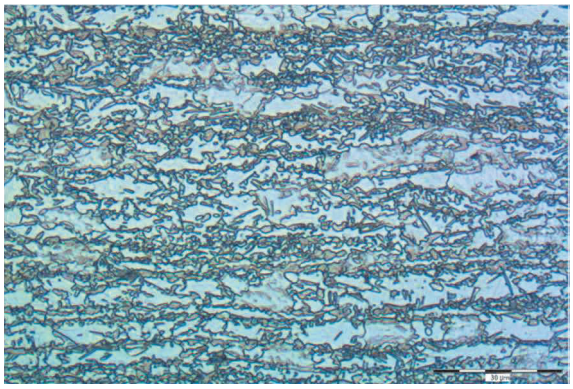

b) Microstructure of TRIP steel Sample B after 10% derormation (LM wih Nital etch)

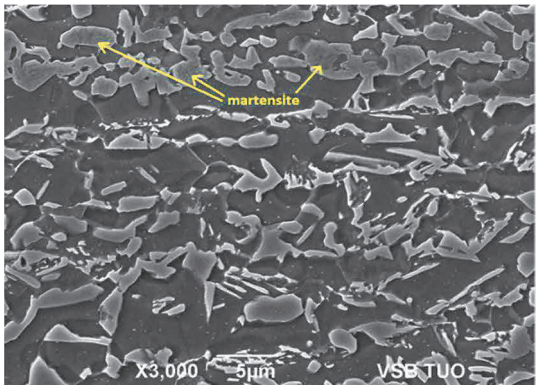

c) Microstructure of TRIP steel Sample C in as-received steel (SEM)

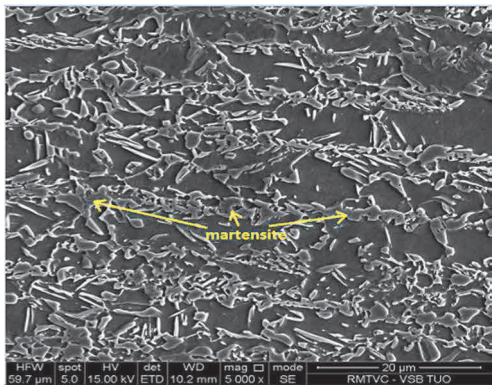

d) Microstructure of TRIP steel Sample B after 10% deformation (SEM)

Figure 2 Microstructure of the TRIP steels

Electrochemical hydrogen permeation tests were carried out using a Devanathan-Stachurski two-component environmental cell consisting of separate charging and oxidation cells constructed from inert materials, with reference electrodes and auxiliary electrodes (usually platinum) and separated by a steel membrane - working electrode. The output side of the membrane was first electroplated with a thin palladium layer, and then mounted between the two cells of the Devanathan-Stachurski setup. The palladium layer serves to prevent

from hydrogen atom recombination during permeation experiments [7]. The processes that occur during the electrochemical permeation of hydrogen are described in **Figure 2**. The hydrogen charging cell was filled with 0.05M H_2SO_4, while the exit cell was filled with 0.1 M NaOH solution. The exit cell was de-aerated by argon bubbling before and during experiments. The hydrogen permeation current was recorded using a VOLTALAB 40 potentiostat during experiments.

After an output current stabilization, the entry side of the specimen was polarized anodically at a current density of + 35 $mA \cdot cm^{-2}$. At the end of this period (5 minutes), H_2SO_4 charging solution was renewed continuously to eliminate metallic ions from the solution. After that, two build-up transients (BUT) were recorded, the first one at the charging current density of -20 $mA \cdot cm^{-2}$, the second one at the charging current density of -35 $mA \cdot cm^{-2}$. Before ending the experiment hydrogen charging was stopped and a decay transient (DT) was also recorded. This procedure was modified with respect to the previous results [9] to shorten the time of experiments and to overcome some disadvantages of the procedure used before. An example of obtained hydrogen permeation curve is shown in **Figure 3.**

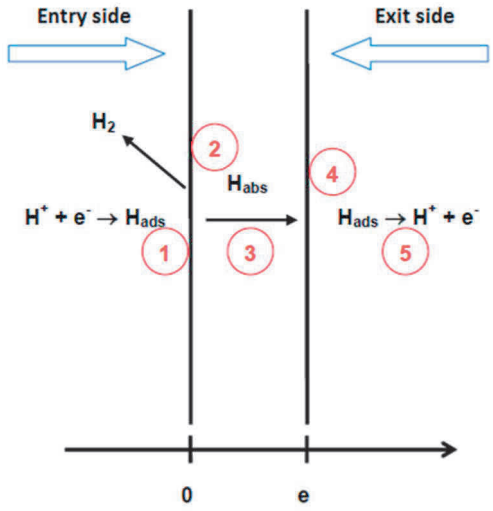

Figure 2 The processes during the electrochemical permeation of hydrogen (1 - reduction of hydrogen from the electrolyte and its adsorption on the steel surface, 2 - absorption of hydrogen, 3 - diffusion of hydrogen through the sample, 4 - hydrogen adsorption on the entry side, 5 - oxidation of hydrogen atoms and their transition into the solution)

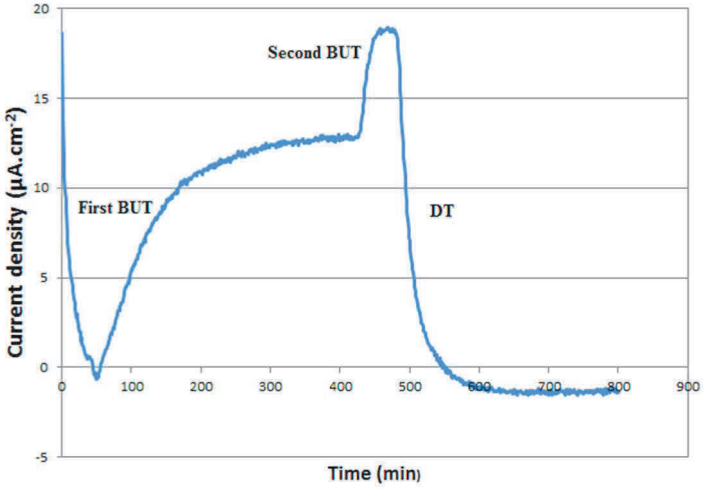

Figure 3 Example of hydrogen permaeation curve for the C-Mn-Si TRIP steel

3. RESULTS AND DISCUSSION

To calculate the effective diffusion coefficient based on the elapsed time, we used the following equation:

$$D_{eff} = \frac{L^2}{6 \cdot t_L} \quad (1)$$

where: L - membrane thickness (cm), t_L- time where the permeation currents reaches 63% of its steady-state value (s).

Sub-surface hydrogen concentration was calculated by **Equation 2**:

$$C_H^0 = \frac{i_\infty \cdot L}{D_{eff} \cdot F} \quad (2)$$

where: i_∞ - steady-state current density ($A \cdot m^{-2}$), L - membrane thickness (m), D_{eff} - effective diffusion coefficient ($m^2 \cdot s^{-1}$), F - Faraday´s constant ($C \cdot mol^{-1}$).

The hydrogen diffusion coefficients are given in **Table 3** for all three studied states and all variants of TRIP steels.

Table 3 Effective hydrogen diffusion coefficient D_{eff} for all studied states and all variants of TRIP steel

State / part of a permeation curve	as-received D_{eff} ($cm^2 \cdot s^{-1}$)			5 % deformation D_{eff} ($cm^2 \cdot s^{-1}$)			10 % deformation D_{eff} ($cm^2 \cdot s^{-1}$)		
	A	B	C	A	B	C	A	B	C
first BUT	$7.49 \cdot 10^{-8}$	$7.50 \cdot 10^{-8}$	$1.80 \cdot 10^{-7}$	$8.10 \cdot 10^{-8}$	$9.00 \cdot 10^{-8}$	$1.48 \cdot 10^{-7}$	$9.32 \cdot 10^{-8}$	$6.76 \cdot 10^{-8}$	$1.50 \cdot 10^{-7}$
second BUT	$4.68 \cdot 10^{-7}$	$4.72 \cdot 10^{-7}$	$6.75 \cdot 10^{-7}$	$6.48 \cdot 10^{-7}$	$5.86 \cdot 10^{-7}$	$7.53 \cdot 10^{-7}$	$6.30 \cdot 10^{-7}$	$4.57 \cdot 10^{-7}$	$8.48 \cdot 10^{-7}$
DT	$2.45 \cdot 10^{-7}$	$2.44 \cdot 10^{-7}$	$4.24 \cdot 10^{-7}$	$3.17 \cdot 10^{-7}$	$2.42 \cdot 10^{-7}$	$4.53 \cdot 10^{-7}$	$3.08 \cdot 10^{-7}$	$2.13 \cdot 10^{-7}$	$5.53 \cdot 10^{-7}$

It can be deduced from **Table 3** that the lowest and nearly the same values of hydrogen diffusion coefficient were obtained for the first BUT in all studied states. This fact can be related to the extensive hydrogen trapping in both reversible and irreversible traps during the 1st BUT. Hydrogen diffusion coefficients corresponding to the 2nd BUT were markedly higher in all states in comparison with the 1st BUT and confirmed thus that the major part of traps was filled by hydrogen during the 1st BUT. In the case of the 2nd BUT hydrogen diffusion coefficient was a little higher for the state after 5 % tensile deformation. This behaviour is in a good agreement with the results of Kim et al. [10]. For the decay transients the hydrogen diffusion coefficients were situated between the values obtained for the 1st and 2nd BUT. All measured values of hydrogen diffusion coefficient for the TRIP Mn-Si and TRIP Mn-Si-Al steel were very low for a predominantly bcc steel and they were even lower in comparison with the values obtained for the TRIP Mn-Si-P, which exhibited the highest values of hydrogen diffusion coefficient in all studied states and for every kind of transient.

Hydrogen sub-surface concentrations were calculated for the 1st BUT using **Equation 2**. The calculated values are rather high for steels having predominantly bcc lattice and they can be attributed to the presence of retained austenite in the structure. The observed increase of the hydrogen sub-surface concentration after tensile deformation can be related to the enhanced hydrogen absorption provoked by the higher dislocation density. On the other hand, the observed values of TRIP Mn-Si and TRIP Mn-Si-Al are lower in comparison with the values calculated for the TRIP Mn-Si-P steel. This difference supports the fact that phosphorus can promote hydrogen absorption into the steel in a significant way. The high sub-surface concentration of hydrogen in the studied TRIP steels can, at least partially, explain rather high susceptibility of the TRIP steels to hydrogen

embrittlement. Hydrogen sub-surface concentrations were only calculated for the 1st BUT. The obtained results are given in **Table 4.**

Table 4 Hydrogen sub-surface concentrations during the first BUT (mass ppm of H)

As-received			5 % tensile deformation			10 % tensile deformation		
A	B	C	A	B	C	A	B	C
11.3	8.6	17.5	13.6	10.9	22.9	15.8	14.1	25.1

4. CONCLUSION

The presented paper was devoted to evaluation and comparison of hydrogen diffusion characteristics in three variants of the TRIP steel. Hydrogen diffusion coefficients of all studied TRIP steels depend only slightly on the steel deformation. The values obtained for the TRIP Mn-Si and TRIP Mn-Si-Al are lower in comparison with TRIP Mn-Si-P, which means that phosphorus can enhance hydrogen diffusion in this steel. Hydrogen sub-surface concentrations are rather high for all studied steels; they increase with the applied tensile deformation. The highest sub-surface concentration was observed in the case of the TRIP C-Mn-P steel, i.e. phosphorus can favor hydrogen adsorption and absorption.

ACKNOWLEDGEMENTS

This paper was created with the contribution of the projects Student Grant Competition SP2017/60 Experimental methods development of the structure and properties of technical materials characterization, and SP2017/58 Specific research in metallurgy, materials and process engineering.

REFERENCES

[1] DE COOMAN, B. C. Structure-properties relationship in TRIP steels containing carbide-free bainite. *Current Opinion in Solid State and Material Science,* 2004, vol. 8, pp 285-303.

[2] DING, W. HEDSTRÖM, P., LI, Y. Heat treatment, microstructure and mechanical properties of aC-Mn-Al-P ho tdip galvanizing TRIP steel. *Mat. Sci. Eng., 2016,* vol. 7, pp.151-157.

[3] VAN SLYCKEN, J. et al. Dynamic response of aluminium containing TRIP steel and its constituent phases. *Mater. Sci. Eng. A*, 2007, vol. 460-461, pp. 516-524.

[4] KLIBER, J., PLESTILOVA, G., ZACEK, O., SOMAN, M. Effects of thermomechanical processing on microstructure and mechanical properties multiphase steels exhibiting a TRIP effect. *Mater. Sci. Forum*, 2007, vol. 539-543, no. 1-5, pp. 4357-4362.

[5] PEREZ ESCOBAR, D. et al.: Internal and surface damage of multiphase steels and pure iron after electrochemical hydrogen charging, *Corr. Sci.*, vol. 53, 2011, pp. 3166-3176.

[6] DEPOVER, T., PEREZ ESCOBAR, D., WALLAERT, E., Zermont, Z., Verbeken, K. Effect of hydrogen charging on the mechanical properties of advanced high strength steels. *Int. J.Hydrogen Energy,* 2014, vol. 39, pp. 4647-4656.

[7] DANIELSON M., J. Use of the Devanathan - Stachurski cell to measure hydrogen permeation in aluminium alloys. *Corr. Sci.*, 2002, vol. 12, pp. 829-840.

[8] SOJKA, J. et al. Effect of hydrogen on the properties and fracture characteristics of TRIP 800 steels. *Corr. Sci.*, 2011, vol. 53, pp. 2575-2581.

[9] SOJKA, J. et al. Hydrogen diffusion in the TRIP 800 steel with higher phosphorus content effect of deformation. In *METAL 2015 : 24th International Conference on Metallurgy and Materials.* Ostrava: TANGER, 2015, 511-516.

[10] KIM, S. J., YUN, D. W., SUH, D. W., KIM, K. Y. Electrochemical hydrogen permeation measurement through TRIP steel under loading condition of phase transition. *Electrochemistry Communications*, 2012, vol. 24, pp. 112-115.